THE JOURNAL OF BIOLOGICAL CHEMISTRY VOL. 289, NO. 15, pp. 10540–10550, April 11, 2014

Sequential Delivery of Synaptic GluA1- and GluA4-containing AMPA Receptors (AMPARs) by SAP97 Anchored Protein Complexes in Classical Conditioning*

Received for publication, November 14, 2013, and in revised form, February 20, 2014 Published, JBC Papers in Press, February 24, 2014, DOI 10.1074/jbc.M113.535179

Zhaoqing Zheng and Joyce Keifer[1]

From the Neuroscience Group, Division of Basic Biomedical Sciences University of South Dakota Sanford School of Medicine, Vermillion, South Dakota 57010

Background: Subunit-specific synaptic delivery of AMPARs during associative learning is not well characterized.
Results: SAP97-AKAP/PKA-GluA1 followed by SAP97-KSR1/PKC-GluA4 complexes function for surface delivery of AMPARs.
Conclusion: SAP97 interacts with AKAP and KSR1 proteins to coordinate the sequential synaptic delivery of AMPAR subunits during *in vitro* classical conditioning.
Significance: A cooperative interaction of multiple scaffolding proteins selectively delivers AMPARs to synapses during conditioning.

Multiple signaling pathways are involved in AMPAR trafficking to synapses during synaptic plasticity and learning. The mechanisms for how these pathways are coordinated in parallel but maintain their functional specificity involves subcellular compartmentalization of kinase function by scaffolding proteins, but how this is accomplished is not well understood. Here, we focused on characterizing the molecular machinery that functions in the sequential synaptic delivery of GluA1- and GluA4-containing AMPARs using an *in vitro* model of eyeblink classical conditioning. We show that conditioning induces the interaction of selective protein complexes with the key structural protein SAP97, which tightly regulates the synaptic delivery of GluA1 and GluA4 AMPAR subunits. The results demonstrate that in the early stages of conditioning the initial activation of PKA stimulates the formation of a SAP97-AKAP/PKA-GluA1 protein complex leading to synaptic delivery of GluA1-containing AMPARs through a SAP97-PSD95 interaction. This is followed shortly thereafter by generation of a SAP97-KSR1/PKC-GluA4 complex for GluA4 AMPAR subunit delivery again through a SAP97-PSD95 interaction. These data suggest that SAP97 forms the molecular backbone of a protein scaffold critical for delivery of AMPARs to the PSD during conditioning. Together, the findings reveal a cooperative interaction of multiple scaffolding proteins for appropriately timed delivery of subunit-specific AMPARs to synapses and support a sequential two-stage model of AMPAR synaptic delivery during classical conditioning.

Numerous protein kinase signaling pathways have been shown to play a critical role in synaptic plasticity mechanisms that underlie learning and memory. A central question is how these pathways are coordinated in parallel and yet maintain their functional specificity during learning. By preassembling components of signaling cascades, molecular scaffolding proteins may influence the efficiency of signaling events to facilitate AMPA receptor (AMPAR)[2] trafficking required for acquisition of learned responses. Intracellular compartmentalization by scaffolding proteins serves to maintain the functional specificity of multiple signaling pathways. Protein kinase A-anchoring proteins (AKAPs) target PKA to distinct subcellular loci and regulate AMPAR surface expression and synaptic plasticity (1–4). Kinase suppressor of Ras1 (KSR1), in contrast, is a scaffold for the Ras/MEK/ERK cascade that facilitates PKC-coupled activation of ERK required for plasticity and memory formation (5). While such scaffolding proteins are key elements of signal transduction pathways their exact function and interactions during synaptic plasticity and learning are not well understood.

Here, we focus on the interaction of several scaffolding proteins that coordinate AMPAR synaptic delivery during acquisition of learned responses using an *in vitro* model of eyeblink classical conditioning. Previously, we proposed a two-stage process for conditioning involving the initial synaptic incorporation of GluA1-containing AMPARs followed by delivery of GluA4 subunits that support acquisition of conditioned responses (CRs; 6–8). Synaptic delivery of GluA1 AMPARs is PKA-dependent while later delivery of GluA4 subunits is NMDAR- and PKC-dependent and requires the first step of GluA1 synaptic incorporation to activate NMDARs in silent synapses. We examined the precise timing of synaptic delivery of specific AMPAR subunits to postsynaptic membranes to determine if they are delivered through different or similar macromolecular signaling complexes. We found that a key

* This work was supported, in whole or in part, by National Institutes of Health Grant NS051187 (to J. K.).
[1] To whom correspondence should be addressed: Neuroscience Group, Basic Biomedical Sciences, University of South Dakota Sanford School of Medicine, 414 E. Clark St., Vermillion, SD 57069. Tel.: 605-677-5134; Fax 605-677-6381; E-mail: jkeifer@usd.edu.

[2] The abbreviations used are: AMPAR, AMPA receptor; AKAP, protein kinase A-anchoring protein; MAGUK, membrane-associated guanylate kinase; TARP, transmembrane AMPAR regulatory protein; CS, conditioned stimulus; US, unconditioned stimulus.

player in AMPAR delivery during conditioning is SAP97, which is a member of the membrane-associated guanylate kinases (MAGUKs) and is involved in organizing protein-protein interactions (9). SAP97 is known to interact directly with GluA1 AMPAR subunits (10) but different scaffolding proteins are thought to interact with other AMPAR subunits (11). How subunit-specific synaptic delivery of AMPARs is achieved has not been well characterized but whether subunit specificity occurs at all has recently been challenged (12). Here, we show that SAP97 interacts with both AKAP and KSR1 protein complexes to coordinate the sequential postsynaptic delivery of GluA1-containing AMPARs followed by GluA4 AMPAR subunits during acquisition of conditioned responding. These findings suggest that SAP97 forms a molecular backbone that coordinates multiple scaffolding proteins for appropriately timed delivery of subunit-specific AMPARs.

EXPERIMENTAL PROCEDURES

Conditioning Procedures—Freshwater pond turtles, *Trachemys scripta elegans*, purchased from commercial suppliers were anesthetized by hypothermia until torpid and decapitated. All experiments involving the use of animals were performed in accordance with the guidelines of the National Institutes of Health and the Institutional Animal Care and Use Committee. The brainstem was transected at the levels of the trochlear and glossopharyngeal nerves, and the cerebellum was removed as described previously (13). The brainstem was continuously bathed in physiological saline (2–4 ml/min) containing (in mM): 100 NaCl, 6 KCl, 40 $NaHCO_3$, 2.6 $CaCl_2$, 1.6 $MgCl_2$, and 20 glucose, which was oxygenated with 95% O_2/5% CO_2 and maintained at room temperature (22–24 °C) at pH 7.6. Suction electrodes were used for stimulation and recording of cranial nerves. The US was a 2-fold threshold single shock applied to the trigeminal nerve while the CS was a 1 s, 100 Hz train stimulus applied to the ipsilateral auditory nerve that was below threshold amplitude required to produce activity in the abducens nerve. Neural responses were recorded from the ipsilateral abducens nerve that innervates the extraocular muscles controlling movements of the eye, nictitating membrane, and eyelid. The CS-US interval was 20 ms, which was defined as the time between the CS offset and the onset of the US. The intertrial interval between the paired stimuli was 30 s. A pairing session was composed of 50 CS-US presentations followed by a 30-min rest period during which no stimuli were delivered. Conditioned responses were defined as abducens nerve activity that occurred during the CS and exceeded an amplitude of 2-fold above the baseline recording level. All treatment groups received paired CS-US stimulation except for pseudoconditioned controls that received the same number of CS and US exposures that were explicitly unpaired using a CS-US interval randomly selected between 300 ms and 25 s.

Pharmacology—The st-Ht31 inhibitor peptide, a stearated form of the Ht31 peptide derived from human thyroid AKAP, or a negative control peptide (Ht31P; Promega, Madison, WI), was added to the physiological saline to a final concentration of 10 μM and applied for 1 h before the conditioning procedure and continued throughout the experiment. The selective membrane-permeable cAMP analog activator of PKA Sp-cAMPs (50 μM), the competitive inhibitor Rp-cAMPs (50 μM; Sigma) or the MEK-ERK inhibitor PD98059 (50 μM; Calbiochem/Millipore) was dissolved in physiological saline and applied to the bath 30 min before the conditioning procedure and continued throughout the experiment. The human SAP97 siRNA or Silencer Negative Control no. 1 siRNA were obtained from commercial suppliers (Ambion, Grand Island, NY). Initial experiments using this siRNA showed that the most effective inhibition of SAP97 protein expression occurred after incubation for 24 h at 100 nM. Therefore, turtle brainstem preparations were incubated with 100 nM anti-SAP97 siRNA or negative control siRNA mixed in Lipofectamine RNAiMAX (Invitrogen) and oxygenated physiological saline for 24 h followed by conditioning. Preparations were frozen in liquid nitrogen for protein analysis.

Coimmunoprecipitation and Western Blot—Immediately after the physiological experiments were performed, brainstem samples for protein analysis were obtained by dissecting a portion of tissue from the pons containing the abducens nuclei only on the stimulated side, frozen in liquid nitrogen, and stored at −80 °C. Brainstems were homogenized in lysis buffer with a protease and phosphatase inhibitor mixture. Protein samples were precleared with protein A/G-agarose, and supernatants were incubated in the primary antibodies or nonspecific rabbit or mouse IgG as a control at 4 °C for 2 h. Protein A/G-agarose was added to the protein samples and incubated at 4 °C overnight. Immunoprecipitated samples or IgG control samples were washed with ice-cold lysis buffer and dissociated by heating for 5 min in the loading buffer and then subjected to SDS-PAGE. For all Western blots and coimmunoprecipitation experiments both input protein and IgG controls were loaded at the same time. The following primary antibodies were used for coimmunoprecipitation and/or Western blotting: SAP97 (EnzoLifeSciences, VAM-PS005), PSD95 (Cell Signaling, 2507), GluA1 (Millipore, 1504), GluA4 (Millipore, 06–308), phospho-ERK (Cell Signaling, 9101), stargazin (Millipore, 9876), total-PKC (Santa Cruz, 10800), KSR1 (Santa Cruz, 9317), AKAP150 (Santa Cruz, 6445), PKA RII (Millipore, 07–1468) and actin for loading controls (Millipore, 1501R). Proteins were detected by the ECL Plus chemiluminescence system (Amersham Biosciences, Piscataway, NJ) or the Odyssey infrared imaging system (Li-Cor Biosciences, Lincoln, NE) and quantified by computer-assisted densitometry.

Biotinylation Assays—Brainstem preparations were incubated in physiological saline containing 1 mg/ml EZ-link sulfo-NHS-LC Biotin (Pierce) and then underwent the conditioning procedure for the required time period. The total elapsed time of incubation in the biotin did not exceed 2 h. At the end of the conditioning procedure, brainstems were washed in ice-cold physiological saline and frozen in liquid nitrogen. Tissue samples were homogenized in lysis buffer (20 mM Tris, pH 8.0, 1 mM EDTA, 1% Nonidet P-40, 0.15 M NaCl, 10 mM $Na_4P_2O_7$, 5% glycine) with a protease (Roche, Germany) and phosphatase inhibitor mixture (Sigma), rotated at 4 °C for 2 h, centrifuged at 14,000 × *g* for 20 min at 4 °C, and the supernatants were stored at −80 °C. Biotinylated proteins (200–300 μg) were incubated with UltraLink Immobilized Streptavidin (Pierce) at 4 °C overnight. Streptavidin-protein complexes were washed with ice-cold washing buffer and pellets were resuspended in 2× SDS/

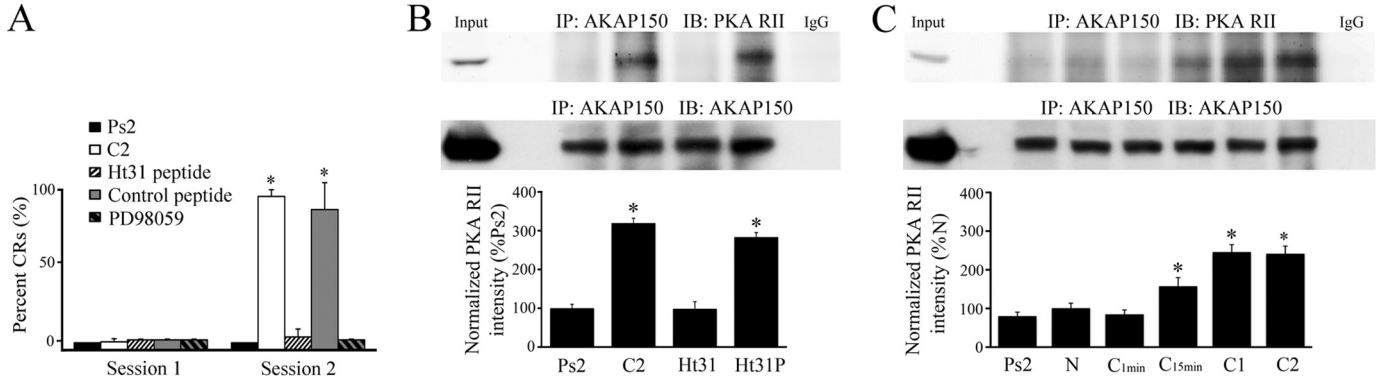

FIGURE 1. **An interaction between PKA and the scaffolding protein AKAP is required for conditioning.** *A*, percent acquisition of CRs in the first and second pairing sessions for preparations that underwent pseudoconditioning for two sessions (*Ps2*), conditioning for two pairing sessions (*C2*), treatment with the PKA inhibitory peptide Ht31 (10 μM), a control peptide (Ht31P, 10 μM), or the MEK-ERK inhibitor PD98059 (50 μM) for two sessions of conditioning is shown. Treatment with Ht31 or PD98059 resulted in no conditioning. *, significant differences from Ps2 ($p < 0.0001$). *B*, immunoprecipitation of AKAP150 with the PKA RII binding domain was greatly enhanced after conditioning at C2. Treatment with the Ht31 peptide during two conditioning sessions disrupted the PKA-AKAP interaction but the control peptide showed little effect compared with normal conditioning. *, significant differences from Ps2. *C*, timing of the onset of the PKA-AKAP protein interaction during conditioning. Significant binding was detected after 15 min of conditioning but not earlier and was maintained throughout the training procedure. Input (whole cell lysates from naïve) and IgG lanes are also shown in *B* and *C*. *N*, naïve untrained preparations, C_{1min}, 1 min of conditioning (2 stimuli), C_{15min}, 15 min of conditioning, C1, one session of conditioning (25 min), C2, two sessions of conditioning (80 min). *, significant differences compared with N, which was 100%. In this and all figures, the *n* and *p* values are given in the text.

β-mercaptoethanol and boiled for 5 min before separation by 10% SDS-PAGE followed by Western blotting. To further confirm the assays only pulled down surface protein, blots were incubated with β-actin and only the whole cell lysis input lane showed a band while the lanes containing biotinylated cell membranes were blank.

Immunocytochemistry, Confocal Imaging, and Data Analysis—After the physiological experiments, brainstems were immersion fixed in 0.5% paraformaldehyde. Tissue sections were cut at 30 μm and preincubated in 10% normal goat serum. Alternate sections were triple labeled with primary antibodies to GluA1, SAP97, and PSD95, or GluA4, SAP97, and PSD95, overnight at 4 °C with gentle shaking. The primary antibodies used were a polyclonal antibody raised in rabbit that recognizes the GluA1 subunit of AMPARs (1:100; Chemicon, 1504), a polyclonal antibody raised in goat that recognizes the GluA4 subunit of AMPARs (1:100; Santa Cruz, 7614), a monoclonal antibody raised in mouse that recognizes PSD95 (1:1000; Thermo Scientific, MA1–046), a polyclonal antibody raised in goat that recognizes the SAP97 (1:1000, Santa Cruz, 26532) or a polyclonal antibody raised in rabbit that recognizes the SAP97 (1:1000; Thermo Scientific, PA1–741). Specificity of the antibodies was confirmed by Western blot. After the primary antibodies, sections were rinsed and incubated with secondary antibodies for 2 h at room temperature. The secondary antibodies were a Cy3-conjugated goat anti-rabbit IgG (1:100) for GluA1 or SAP97, a Cy5-conjugated rabbit anti-goat IgG (1:100) for GluA4 or SAP97 (Jackson ImmunoResearch, West Grove, PA), and an Alexa Fluor 488-conjugated goat anti-mouse IgG (1:100) for PSD95 (Invitrogen). The sections were rinsed, mounted on slides, and coverslipped. Images of labeled neurons in the principal and accessory abducens motor nuclei (15 cells/preparation) were obtained using an Olympus Fluoview 1000 laser scanning confocal microscope. Tissue samples containing abducens motor neurons were scanned using a 60 × 1.4 NA oil-immersion objective with triple excitation with a 488-nm argon laser, a 543-nm HeNe laser, and a 635-nm diode laser. Quantification of punctate staining of abducens neuronal somata and dendrites that was at least 2-fold greater intensity above background was performed using stereological procedures (14) with MetaMorph software (Universal Imaging, Downingtown, PA). Images of two consecutive optical sections were taken using confocal microscopy. Protein puncta were counted in one optical section (sample section) if they were not present in the optical section immediately below the sample section (look-up section), and if they were within the inclusion boundaries of the unbiased counting frame. Colocalized staining was determined when puncta were immediately adjacent to one another or if they were overlapping.

Statistics—All data were analyzed using a one-way ANOVA followed by *post hoc* analysis using Fisher's and Bonferroni tests and are presented as means ± S.E. *P* and *n* values are given in the text where *n*'s represent the number of brainstem preparations.

RESULTS

Enhanced Interaction of SAP97-AKAP/PKA-GluA1 in Early Conditioning Results in Synaptic Delivery of GluA1—Our previous experiments showed that phosphorylation of PKA has a critical role in initiating the signaling cascade required for classical conditioning (6). PKA activation leads to rapid NMDAR-independent synaptic delivery of GluA1-containing AMPARs and later NMDAR-dependent synaptic trafficking of GluA4 subunits that underlie acquisition of CRs. To test whether an interaction with the scaffolding protein AKAP is necessary for PKA to initiate conditioning, the association between PKA and AKAP was perturbed using the Ht31 peptide. Ht31 is a cell-permeable peptide that contains the critical RII-binding domain and disrupts PKA-AKAP interactions (15). Pretreatment of brainstem preparations with 10 μM Ht31 significantly inhibited the acquisition of conditioning that normally occurs in the second pairing session (C2; Fig. 1*A*, $n = 6$/group; $p < 0.0001$, C2 *versus* Ht31). Further, coimmunoprecipitation studies showed that the association between PKA and AKAP was

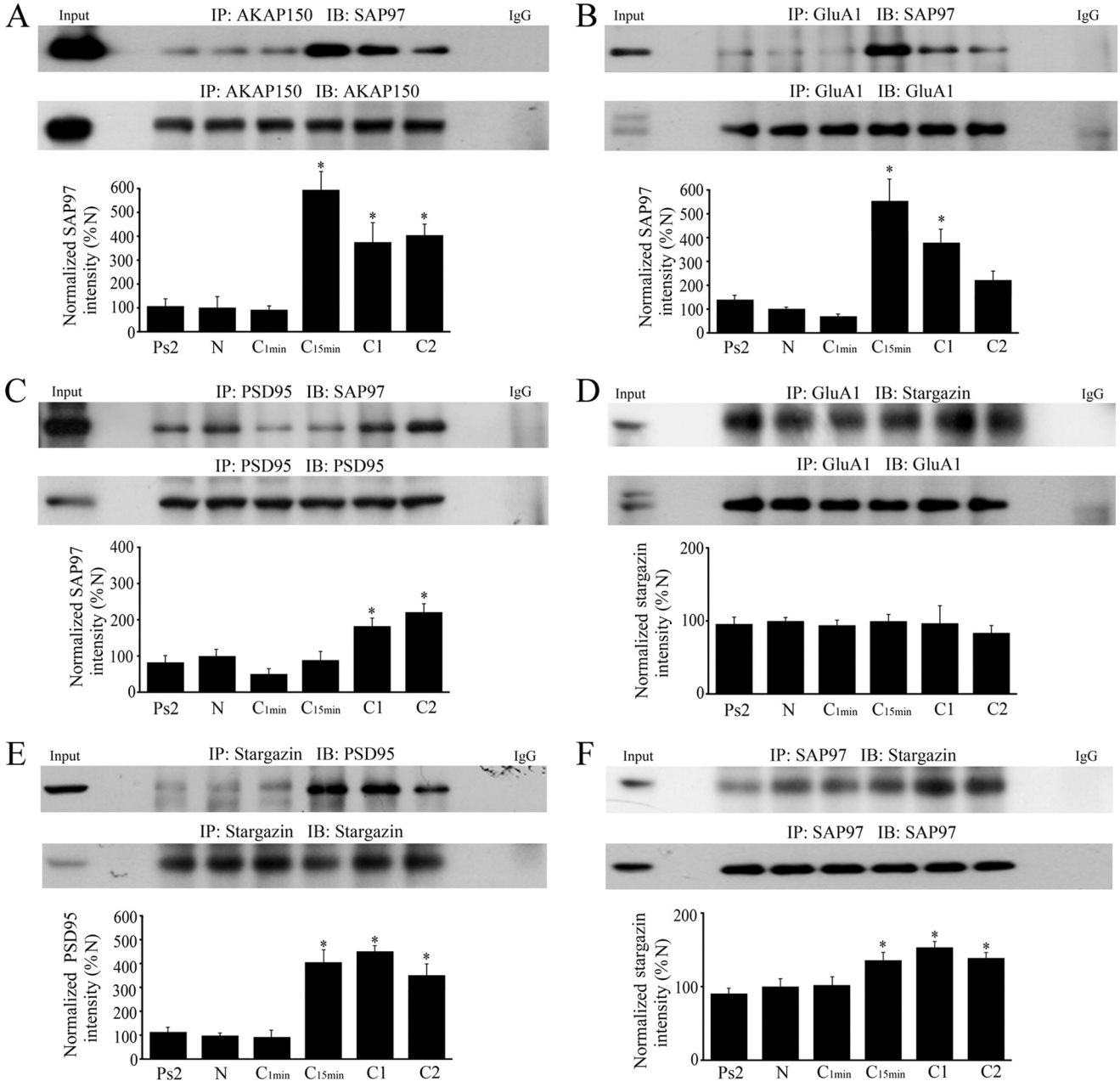

FIGURE 2. **A SAP97-AKAP-GluA1 protein complex forms early in conditioning and is delivered to PSD95 as shown by coimmunoprecipitation studies.** *A–F*, analysis of the timing of the protein-protein interactions induced by conditioning evaluated in naïve, pseudoconditioned, and conditioned preparations that underwent training for the different time periods indicated is shown. Except for the GluA1-stargazin (*D*) association that failed to show conditioning-related changes, significant interactions were observed mainly after 15 min of conditioning. Input (naïve) and IgG lanes are also shown. *, significant differences from N.

disrupted compared with normal conditioning at C2 (Fig. 1*B*, $n = 6$/group; $p < 0.0001$, C2 *versus* Ht31). However, both conditioning and the PKA-AKAP interaction were unaffected when preparations were incubated with a negative control peptide (Fig. 1*B*, *Ht31P*). The time course of the association between PKA and AKAP was further explored by coimmunoprecipitation experiments (Fig. 1*C*). This interaction was significantly enhanced during conditioning for 15 min ($n = 6$/group; $p = 0.005$, N *versus* C_{15min}) and remained at high levels through two sessions of conditioning ($p < 0.0001$, N *versus* C2). Therefore, the anchoring of PKA to AKAP occurs early during conditioning and is required for acquisition of CRs.

Next, using coimmunoprecipitation we examined how AKAPs serve to target PKA to distinct subcellular loci and coordinate multiple signaling enzymes in supramolecular complexes to mediate synaptic AMPAR trafficking. We first investigated the interaction between AKAP and SAP97. At 15 min of conditioning AKAP and SAP97 showed strong binding (Fig. 2*A*, $n = 4$/group; $p < 0.0001$, N *versus* C_{15min}) although this interaction was weakened slightly with further conditioning but remained at significantly high levels compared with the naïve group ($p = 0.007$, N *versus* C2). We further discovered that SAP97 forms a complex with GluA1 also after 15 min of conditioning (Fig. 2*B*, $n = 4$/group; $p < 0.0001$, N *versus* C_{15min}),

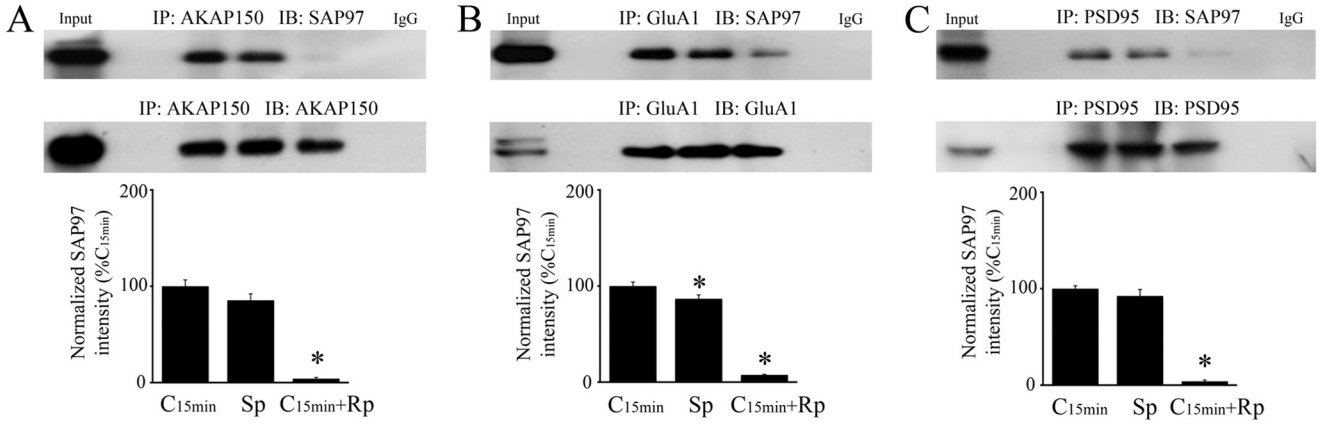

FIGURE 3. **Activation of PKA is involved in SAP97-AKAP-GluA1 complex formation and delivery to PSD95.** *A–C*, coimmunoprecipitation analysis was performed on preparations that were conditioned for 15 min or were treated for the equivalent time period with the PKA analog Sp-cAMPs (50 μM) applied alone or application of the antagonist Rp-cAMPs (50 μM) during conditioning. Sp-cAMPs alone induced an interaction of SAP97 protein with AKAP (*A*), GluA1 AMPAR subunits (*B*), and PSD95 (*C*) similar to normal conditioning while Rp-cAMPs significantly inhibited these associations. Input (naïve) and IgG lanes are also shown. *, significant differences from C_{15min}.

which gradually dissociated with longer training ($p = 0.16$, N *versus* C2). Shortly after these associations with SAP97 were detected, a significant interaction between SAP97 and PSD95 was observed after one training session of conditioning (C1) or after 25 min (Fig. 2*C*, $n = 6$/group; $p = 0.004$, N *versus* C1), and this interaction was maintained through two pairing sessions ($p < 0.0001$, N *versus* C2). Because it has a known role in AMPAR trafficking, we next examined stargazin (γ2), a transmembrane AMPAR regulatory protein (TARP) that facilitates AMPAR clustering and synaptic targeting. Unlike SAP97, the interaction between GluA1 and stargazin did not show significant conditioning-related changes (Fig. 2*D*, $n = 6$; $p = 0.80$). In contrast, however, the association between stargazin and PSD95 was significantly augmented at 15 min and throughout conditioning (Fig. 2*E*, $n = 6$; $p < 0.0001$, N *versus* C_{15min}). This was associated with a concomitant modest but significant increase in the interaction between SAP97 and stargazin (Fig. 2*F*, $n = 6$; $p = 0.03$). Together, these data suggest that ~15 min after the onset of conditioning a SAP97-AKAP/PKA-GluA1 complex forms that is delivered to PSD95 within 25 min at C1 through a SAP97-PSD95 interaction. Stargazin appears to be bound continuously to GluA1, and its immunoprecipitation pattern reflects linkages with SAP97 and delivery to PSD95 during conditioning.

To further confirm that activation of PKA is involved in SAP97-AKAP/PKA-GluA1 complex formation and delivery to PSD95, the selective PKA activator Sp-cAMPs (50 μM) or competitive inhibitor Rp-cAMPs (50 μM) were applied. As shown in Fig. 3, incubation of preparations in Sp-cAMPs alone induced strong interactions among SAP97 and AKAP, GluA1 and PSD95 compared with conditioning for 15 min (Fig. 3, *A–C*, $n = 3$/group, N.S., C_{15min} *versus* Sp, except for GluA1:SAP97, which was slightly less than conditioning at $p = 0.01$). All of these interactions were blocked by application of the PKA inhibitor Rp-cAMPs during conditioning (Fig. 3, *A–C*, $p < 0.0001$, Sp *versus* Rp all panels). These findings confirm that formation of a SAP97-AKAP/PKA-GluA1 complex to regulate AMPAR synaptic delivery during conditioning is dependent on initial PKA activation.

The contribution of SAP97 to GluA1 synaptic delivery during conditioning was assessed by using a SAP97 siRNA and detection of membrane surface expression of GluA1 using the biotinylation assay. During conditioning, surface expression of GluA1 was significantly increased after 15 min of pairing and remained high after C1 or 25 min (Fig. 4*A*, $n = 4$/group; $p < 0.01$, N *versus* C_{15min}). By two sessions of conditioning at C2, surface levels of GluA1 declined back to naïve values ($p = 0.45$, N *versus* C2). GluA1 subunits do not undergo protein synthesis during conditioning but surface GluA1 increased 477% at C_{15min} compared with surface naïve. This was an average ratio of surface over total of 14% at C_{15min} from 9% for naïve ($p = 0.001$). Preincubation of preparations by bath application of an siRNA directed against SAP97 for 24 h followed by conditioning for one session resulted in a significant reduction in SAP97 protein expression to 59% percent of the value obtained during conditioning in a negative control siRNA (Fig. 4*B*, $n = 4$/group; $p < 0.0001$, C1+NCsiRNA *versus* C1+SAP97siRNA). This level of SAP97 knockdown appeared to be enough to interfere with both the immunoprecipitation of SAP97 with PSD95 by 57% (Fig. 4*C*, $n = 4$; $p = 0.004$) and, importantly, resulted in inhibition of the surface delivery of GluA1 during SAP97 siRNA treatment (Fig. 4*D*, $n = 4$; $p = 0.01$; surface/total GluA1 was 13% in NC siRNA and fell to 10% in SAP97 siRNA, $p = 0.0004$). Collectively, these findings strongly support the conclusion that the formation of a SAP97-AKAP/PKA-GluA1 complex is involved in GluA1 AMPAR membrane insertion at synapses during the early stages of conditioning.

A SAP97-KSR1/PKC-GluA4 Complex Delivers Synaptic GluA4 Later in Conditioning—In our model of classical conditioning, the initial synaptic incorporation of GluA1-containing AMPARs to activate silent auditory nerve synapses onto abducens motoneurons is followed by delivery of GluA4 subunits that support acquisition of CRs (8). The later phase of GluA4 AMPAR synaptic incorporation is mediated by activation of PKC and ERK (16). Here, we investigated the scaffolding partners that mediate GluA4-containing AMPAR trafficking. KSR1 is a scaffolding protein and positive effector for the Raf/MEK/ERK kinase cascade (17–18) and specifically facilitates activa-

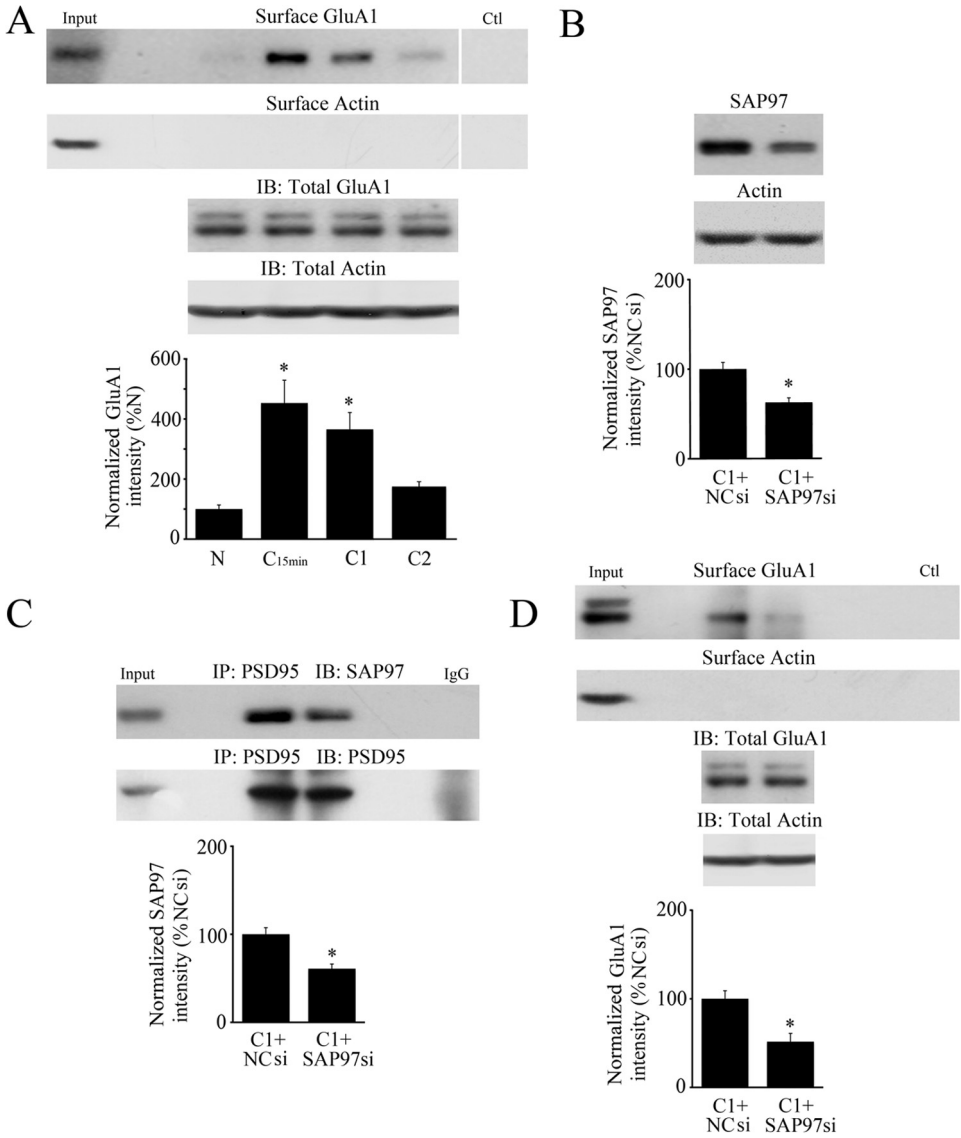

FIGURE 4. **Delivery of surface GluA1-containing AMPARs during conditioning is inhibited by an siRNA directed against SAP97.** *A*, surface expression of GluA1 AMPAR subunits is detected by Western blotting after 15 min of conditioning and is maintained through one session of conditioning at C1, but levels decline to naïve values by C2. Surface actin is also shown as are total GluA1 and actin protein from lysates. *, significant differences from N. *B*, administration of a SAP97 siRNA to the bath for 24 h resulted in significant knockdown of SAP97 protein expression during conditioning compared with conditioning in a negative control siRNA (NCsi). *C*, after treatment with SAP97 siRNA, immunoprecipitation of PSD95 with SAP97 during conditioning was reduced compared with conditioning in the control siRNA. *D*, surface expression of GluA1-containing AMPARs was inhibited by the SAP97 siRNA treatment during conditioning showing that SAP97 has an important role in GluA1 trafficking. Surface actin is also shown as are total GluA1 and actin protein from lysates. Input lanes are whole cell lysates from naive. In *A* and *D*, the control (*Ctl*) lane is a whole cell lysis sample without biotin treatment. *B–D*, *, significant differences from C1 + NCsi.

tion of a membrane pool of ERK that is preceded by activation of PKC (5). During conditioning, we observed that KSR1 immunoprecipitates with SAP97 after one and two sessions of pairing (Fig. 5*A*, $n = 4$/group; $p < 0.0001$, N *versus* C1 or C2). At the same time, GluA4-containing AMPAR linkages with SAP97 are also recruited (Fig. 5*B*, $n = 4$/group; $p < 0.0001$, N *versus* C1 or C2) suggesting the formation of a SAP97-KSR1-GluA4 protein complex. Similar to GluA1 subunits, stargazin interacts with GluA4 but not in an activity-dependent manner (Fig. 5*C*, $n = 6$/group; $p = 0.37$, all groups). Additionally, we observed that both PKC and p-ERK were recruited to KSR1 in the later stage of conditioning at C2 (Fig. 5*D*, $n = 6$/group; $p = 0.0003$; Fig. 5*E*, $n = 6$/group; $p < 0.0001$, N *versus* C2). A potent and selective inhibitor of MEK, PD98059 (50 μM), not only completely inhibited conditioning (Fig. 1*A*) but also interfered with the p-ERK-KSR1 interaction (Fig. 5*F*, $n = 6$/group; $p < 0.0001$, C2 *versus* PD98059) while this binding was induced by the PKA activator Sp-cAMPs (50 μM) when applied alone (Fig. 5*F*, $p < 0.0001$, Ps2 *versus* Sp-cAMPs). These data suggest that the scaffolding protein KSR1 facilitates targeting of GluA4-containing AMPARs to synapses in later stages of conditioning. It appears that SAP97 binds KSR1 and GluA4 at the same time it also shows high levels of interaction with PSD95 (Fig. 2*C*). Therefore, the SAP97-KSR1-GluA4 complex serves as a backbone for the kinase activity of PKC and ERK by recruiting these elements to synapses.

To directly test whether disrupting SAP97 has an effect on GluA4 trafficking we again used the SAP97 siRNA and AMPAR biotinylation assay. The level of surface GluA4 gradually

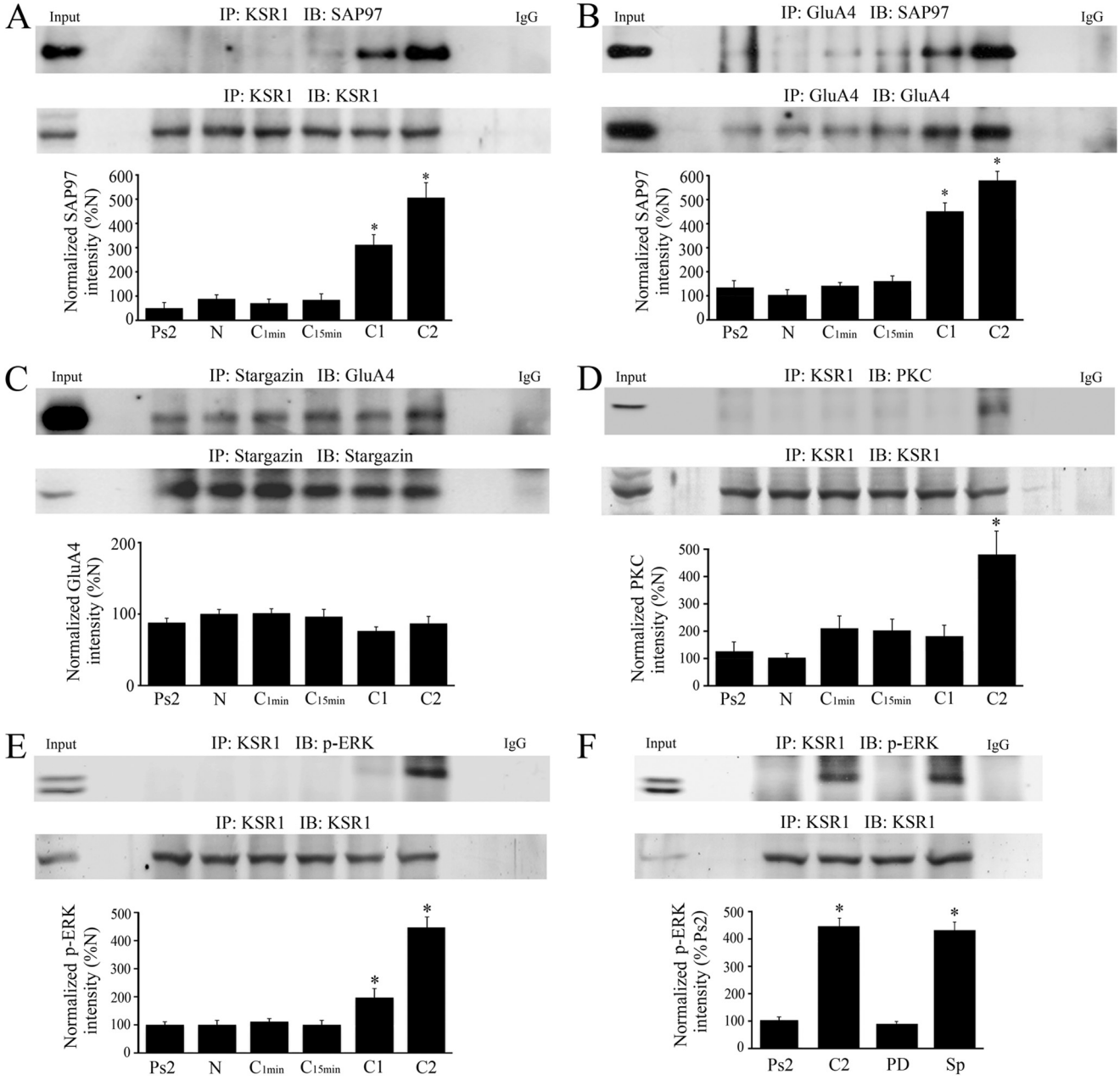

FIGURE 5. **A SAP97-KSR1-GluA4 protein complex forms later in conditioning and interacts with protein kinases PKC and ERK.** *A–E*, coimmunoprecipitation analysis of the timing of the protein-protein interactions induced by conditioning was evaluated in naïve, pseudoconditioned, and conditioned preparations that underwent training for the different time periods indicated. Except for the GluA4-stargazin (*C*) association that did not demonstrate conditioning-related changes, significant interactions were observed during conditioning beginning at C1 or C2. Input (naïve) and IgG lanes are also shown. *, significant differences from N. *F*, conditioning-dependent immunoprecipitation of KSR1 with p-ERK was inhibited by the MEK-ERK blocker PD98059 (50 μM) and stimulated by application of the PKA activator Sp-cAMPs (50 μM). *, significant differences from Ps2.

increased in the later stages of conditioning starting at C1 and was significantly increased at C2 or after 80 min (Fig. 6*A*, n = 4/group; $p < 0.0001$, N *versus* C2). GluA4 subunits undergo protein synthesis during conditioning to just over double naïve values in C2 (207%). The ratio of surface to total GluA4 protein peaked at 9% in C2 from 4% in naive ($p = 0.001$) indicating that GluA4 membrane insertion had occurred. These values for surface/total AMPAR ratio are likely to be an underestimate because the abducens motor neurons that undergo conditioning are embedded in additional brainstem tissue. Similar to data for one session of pairing (Fig. 4*B*), application of SAP97 siRNA resulted in a 44% knockdown of SAP97 protein after two sessions of conditioning (Fig. 6*B*, n = 4/group; $p = 0.001$). Significantly, knockdown of SAP97 resulted in a 49% reduction in the association of SAP97 with PSD95 (Fig. 6*C*, n = 4/group; $p < 0.0001$) and subsequent inhibition of surface expression of GluA4-containing AMPARs (Fig. 6*D*, n = 4/group; $p = 0.01$; surface/total GluA4 was 8% in NC siRNA and fell to 5% in SAP97 siRNA, $p < 0.05$). In these cases, an average of 0% CRs were recorded.

Visualization of Protein Complexes Involved in Synaptic Delivery of AMPARs—Confocal imaging of immunocytochemically stained abducens motor neurons was performed to con-

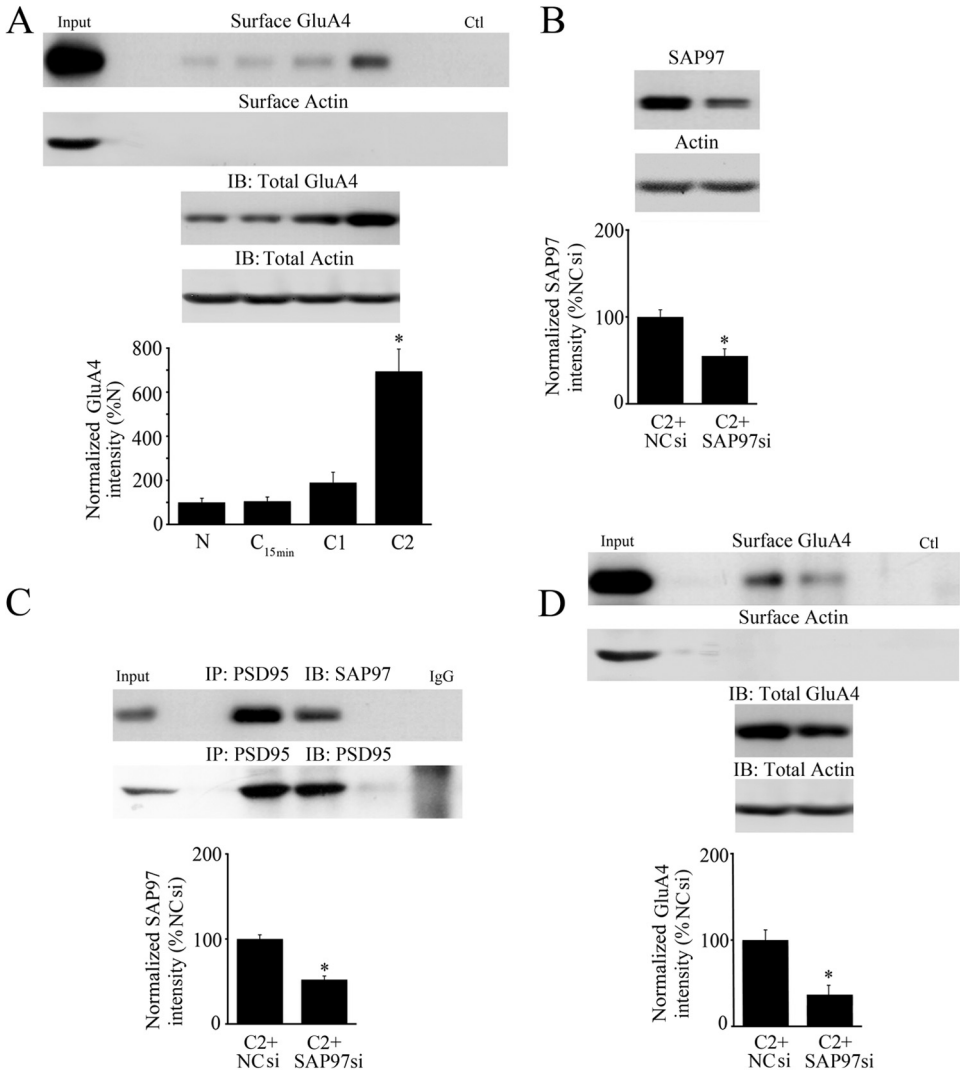

FIGURE 6. **Delivery of surface GluA4-containing AMPARs occurs later in conditioning than GluA1 and is also inhibited by an siRNA directed against SAP97.** *A*, surface expression of GluA4 AMPAR subunits was detected after two sessions of conditioning (80 min). Surface actin is also shown as are total GluA4 and actin protein from lysates. *, significant differences from N. *B*, administration of a SAP97 siRNA for 24 h resulted in knockdown of SAP97 protein expression during two sessions of conditioning compared with conditioning in a negative control siRNA (*NCsi*). *C*, after treatment with SAP97 siRNA, immunoprecipitation of SAP97 with PSD95 during two sessions of conditioning was greatly reduced compared with conditioning in the control siRNA. *D*, surface expression of GluA4-containing AMPARs was inhibited by SAP97 siRNA treatment during conditioning showing that SAP97 has a role in trafficking of GluA4-containing AMPARs. Surface actin is also shown as are total GluA4 and actin protein from lysates. Input lanes are whole cell lysates from C2. In *A* and *D*, a greater concentration of GluA4 antibody was used for surface GluA4 compared with the westerns for total GluA4 to obtain clear bands; the control (*Ctl*) lane is a whole cell lysate sample without biotin treatment. *B–D*, *, significant differences from C2+NCsi.

firm sequential delivery of synaptic GluA1- followed by GluA4-containing AMPARs during conditioning. Images of punctate staining for AMPARs and postsynaptically localized scaffolding proteins for the different experimental groups are shown in Fig. 7 ($n = 3$/group, 45 neurons/group). Consistent with the coimmunoprecipitation findings (Fig. 2*C*), colocalization of SAP97 with PSD95 significantly increased after one session of conditioning to 155% above naïve preparations (Fig. 7*A*; $p < 0.0001$), and this was slightly enhanced to 165% after two sessions of conditioning ($p < 0.0001$). Corresponding with assembly of SAP97-PSD95 protein interactions, triple-label colocalization of GluA1 AMPAR subunits with SAP97 and PSD95 was observed to be increased to 244% above naïve levels after conditioning for one session (Fig. 7*B*; $p < 0.0001$) suggesting that a GluA1-SAP97 linkage was established and GluA1 was delivered to the PSD. However, after two sessions, triple-label colocalization declined to control values due to a loss of GluA1 (Fig. 7*B*) while SAP97-PSD95 colocalization remained high (Fig. 7*A*). These observations from the imaging are consistent with our findings showing considerably less immunoprecipitation of GluA1 with SAP97 after C2 (Fig. 2*B*). Parallel to the findings for GluA1 after one conditioning session, colocalization of GluA4-containing AMPARs with SAP97 and PSD95 also markedly increased compared with naïve (Fig. 7*C*; $p = 0.0003$) consistent with the coimmunoprecipitation findings (Fig. 5*B*). Triple-label colocalization of GluA4-SAP97-PSD95 continued to increase after two sessions of conditioning to 234% above naïve values ($p < 0.0001$) in the same time frame that the peak surface GluA4 level was observed (Fig. 6*A*) suggesting synaptic delivery of GluA4 AMPAR subunits had occurred. These immunocytochemical observations provide strong support for our biochemical evidence that a SAP97-PSD95 complex forms and is main-

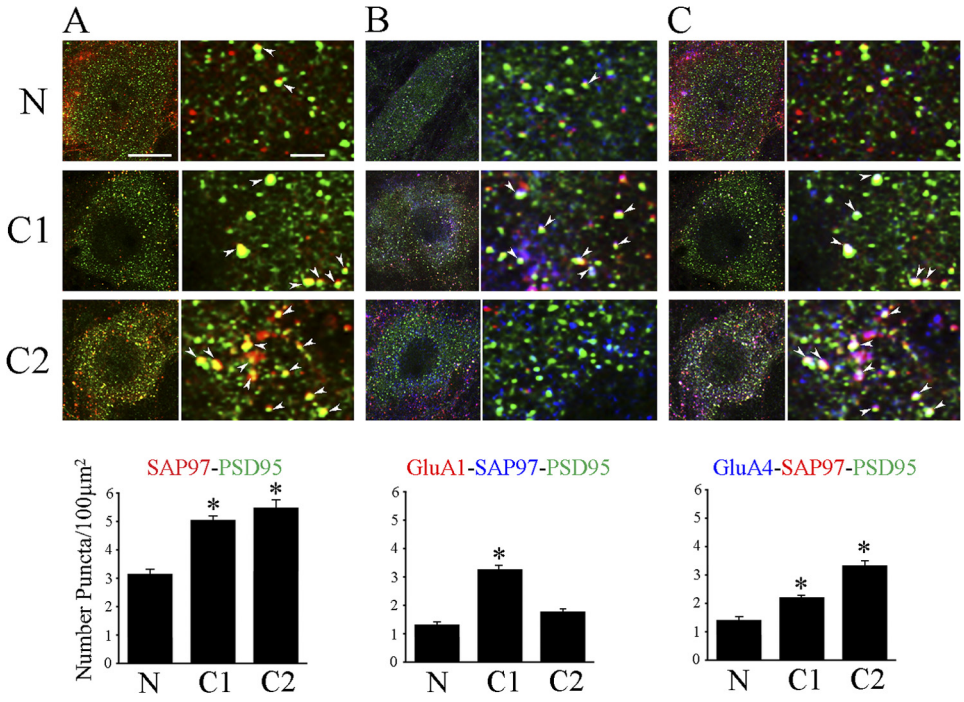

FIGURE 7. **Visualization of protein colocalization in abducens motor neurons by immunostaining and confocal microscopy.** Images of labeled neurons are shown to the left of each panel and higher power magnification of punctate staining is shown at right for each experimental group. Quantitative analysis of punctate staining using stereological procedures is shown below. *A*, colocalization of SAP97 (*red*) and PSD95 (*green*) was significantly increased after conditioning for C1 and C2 compared with naïve preparations. Colocalization is shown as yellow staining and is indicated by the *arrowheads*. *B*, triple-label colocalization of GluA1 (*red*), SAP97 (*blue*), and PSD95 (*green*) increased greatly at C1 but then declined to naïve values at C2. The decline at C2 was due to loss of GluA1 punctate staining as there was ample colocalization of SAP97-PSD95 (see *A*), which appears as light blue staining in the *lowest image panel* in *B* for C2. *C*, triple-label colocalization of GluA4 (*blue*), SAP97 (*red*), and PSD95 (*green*) was also observed to increase at C1 but this staining was further increased at C2 and is shown as white staining. *, significant differences from N. Scale bars, 10 μm in panels to the *left*, 2 μm in panels to the *right*.

tained during synaptic delivery of GluA1-containing AMPARs in C1 followed by later delivery of GluA4-containing AMPARs in C2, and that this process occurs in the abducens motor neurons.

DISCUSSION

Postsynaptic regulation of AMPARs has emerged as one of the fundamental concepts in understanding the underlying mechanisms of learning and memory. Timed interactions among specific scaffolding proteins and kinases with AMPARs are important elements for their proper subcellular localization and function. Our previous studies indicated that PKA-mediated synaptic incorporation of GluA1-containing AMPARs is required to unsilence auditory nerve synapses followed by an NMDAR- and PKC-dependent signaling process for the later delivery of GluA4-subunits required for acquisition of CRs (6, 8, 16). Synaptic delivery of AMPARs with different subunit composition raises the possibility that distinct molecular machineries are used. In the present study, we found that conditioning induces the formation of selective protein complexes with the key structural protein SAP97 which coordinates the sequential synaptic delivery of GluA1- and GluA4-containing AMPARs. Our results demonstrate that in the early stages of conditioning the initial activation of PKA stimulates the formation of a SAP97-AKAP/PKA-GluA1 protein complex leading to synaptic delivery of GluA1 AMPARs through a SAP97-PSD95 interaction. This is followed shortly thereafter by a SAP97-KSR1/PKC-GluA4 complex for GluA4 AMPAR delivery again through a SAP97-PSD95 interaction. These data indicate that SAP97 forms the backbone of a dynamic protein scaffold that functions in the sequential delivery of specific AMPAR subunits to the PSD during classical conditioning.

Appropriately timed activation of multiple signaling pathways are involved in AMPAR trafficking during *in vitro* classical conditioning including PKA, PKC, ERK, and NMDAR activation (6, 7, 16, 19). The mechanisms for how these signaling pathways are coordinated in parallel but maintain their functional specificity is just beginning to be described. In the case of classical conditioning here, our evidence suggests that the MAGUK SAP97 has a central role in organizing other scaffolding proteins and kinases for delivery of AMPARs to the PSD. Based on our data, the following model was constructed to describe this process and to guide further experiments (Fig. 8). Phosphorylation and targeting of GluA1-containing AMPARs by PKA is facilitated by the anchoring protein AKAP and disruption of the PKA-AKAP interaction has previously been shown to impede LTP and spatial learning (1, 2, 4). We found that the PKA RII subunit binds to AKAP as early as 15 min after conditioning onset and that disruption of this interaction by the Ht31 peptide results in inhibition of conditioning (Fig. 1). Further analysis of AKAP shows that it binds to SAP97 in a PKA- (Fig. 3*A*) and conditioning-dependent (Fig. 2*A*) manner, an interaction that has been observed previously (1). SAP97 is known to directly bind to GluA1 AMPAR subunits (10), and this was also observed here but this association is conditioning-dependent (Fig. 2*B*). Together, these data show that a SAP97-AKAP/PKA-GluA1 protein complex is formed 15 min after

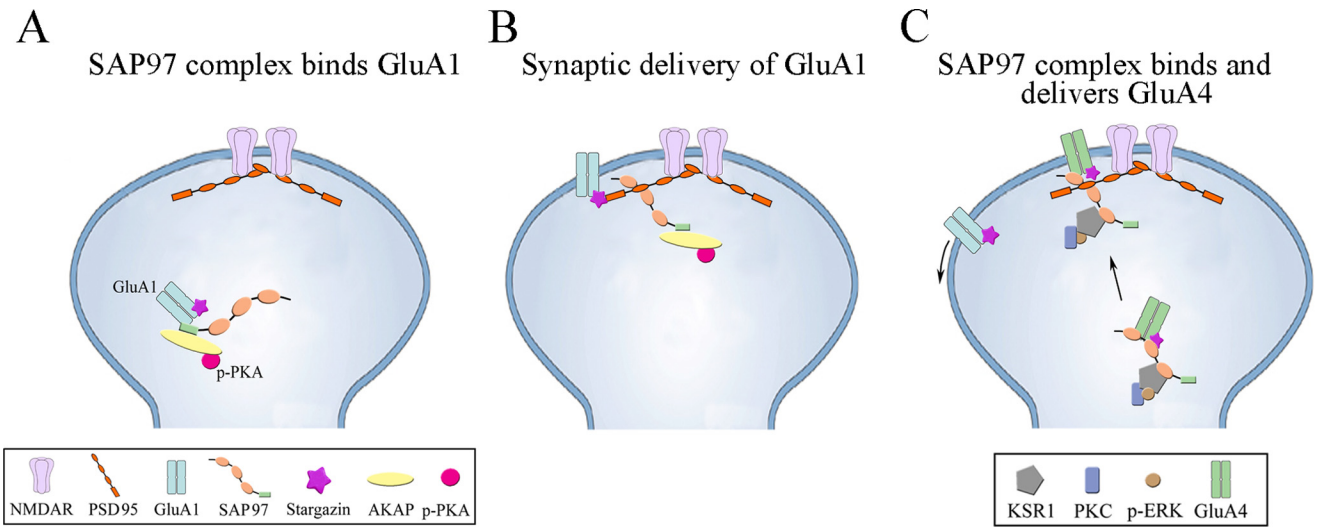

FIGURE 8. **Model summarizing our findings on the role of SAP97 and other scaffolding proteins and kinases on subunit-specific synaptic delivery of AMPARs during early and later stages of *in vitro* classical conditioning.** *A*, about 15 min after conditioning onset, a SAP97-AKAP/PKA-GluA1 protein complex forms that is initiated by the phosphorylation of PKA. *B*, shortly after *A* at about C1 (25 min), this complex translocates to the PSD where there is an interaction between SAP97-PSD95 and GluA1-containing AMPARs are released from SAP97 for delivery to the synapse. *C*, still later in conditioning at about C2 (80 min after conditioning onset), a SAP97-KSR1/PKC-GluA4 complex forms. This occurs while SAP97 is already bound to PSD95 and/or there are new SAP97 complexes that translocate to the PSD to deliver GluA4 AMPAR subunits to the synapse. This step requires the phosphorylation of ERK. During this phase GluA1-containing AMPARs are removed from the membrane surface.

conditioning onset and is maintained into C1 of conditioning (25 min). Additionally, stargazin, which associates with GluA1 AMPARs independently of conditioning, is also part of the complex. These protein-protein interactions after 15 min of conditioning are illustrated in Fig. 8*A*. From our coimmunoprecipitation timing data, it appears that shortly after the formation of this complex it is delivered to the PSD which is indicated by a significantly enhanced SAP97-PSD95 interaction at C1 (Fig. 2*C*). These findings are corroborated by the immunocytochemical data showing greater colocalization of SAP97-PSD95 on abducens motor neurons at C1 (Fig. 7*A*). We suggest this process results in the synaptic insertion of GluA1-containing AMPARs into the PSD as is indicated by the enhanced surface expression of GluA1 subunits at C1 (Fig. 4*A*). Significantly, both the SAP97-PSD95 interaction and surface expression of GluA1 are inhibited by an siRNA directed against SAP97 (Fig. 4, *B–D*) demonstrating the significant role of SAP97 for GluA1 AMPAR trafficking in conditioning. The process of GluA1 synaptic delivery is illustrated in Fig. 8*B*. One interesting sidelight to these data is that greatly increased surface expression of GluA1 occurs 15 min after conditioning (Fig. 4*A*) while significantly increased immunoprecipitation of PSD95 with SAP97 is not observed until C1 (Fig. 2*C*). One possibility to explain this apparent discrepancy is that GluA1-containing AMPARs are initially delivered to the extrasynaptic membrane by SAP97 in 15 min and are translocated into the PSD slightly later at C1. Supporting this idea, delivery of AMPARs to extrasynaptic sites shortly after LTP induction has been previously observed and is thought to precede full-scale synaptic potentiation (20–22). This issue remains to be resolved for *in vitro* classical conditioning. Interestingly, a SAP97-AKAP complex also contributes to β1-adrenergic receptor recycling and is involved in targeting PKA to this receptor (15). Thus, MAGUK-mediated trafficking of synaptic proteins might be a common mechanism involved in activity-dependent translocation of postsynaptic receptors.

Synaptic insertion of GluA4-containing AMPARs during conditioning requires the first step of GluA1 AMPAR incorporation to unsilence auditory nerve synapses on abducens motor neurons by activating NMDARs (6). This is a PKC-dependent process that uses several conventional and atypical PKC isoforms (6, 16, 19). Our data indicate that the MEK-ERK scaffold KSR1 shows markedly increased immunoprecipitation with SAP97 during conditioning at C1 which increases further at C2 (Fig. 5*A*) and PKC shows a dramatically increased interaction with KSR1 at C2 (Fig. 5*D*) as well as p-ERK (Fig. 5*E*). Concomitantly, GluA4 AMPAR subunits demonstrate a strong interaction with SAP97 starting at C1 that increases in C2 (Fig. 5*B*) while at the same time GluA1 subunits show a weaking interaction (Fig. 2*B*). These data suggest that a SAP97-KSR1/PKC-GluA4 protein complex is formed during conditioning at about C1 and is maintained into C2. Similar to GluA1, the association of stargazin with GluA4 AMPARs is independent of conditioning but is also part of this complex, which is illustrated in Fig. 8*C*. We postulate that this complex, consisting of SAP97 with new binding partners, translocates to or is already present within the PSD to deliver GluA4-containing AMPARs in later stages of conditioning. Correspondingly, surface GluA4 AMPARs increase dramatically at C2 (Fig. 6*A*), which is substantiated by the immunocytochemical observations of protein colocalization on abducens motor neurons (Fig. 7*C*). GluA4 subunits undergo protein synthesis and we observed a corresponding increase in surface GluA4 expression. This might indicate that newly synthesized GluA4 subunits are inserted into the membrane during conditioning. Inhibition of surface GluA4 and the SAP97-PSD95 interaction by the SAP97 siRNA confirms the significant role of SAP97 in GluA4 subunit delivery during conditioning at C2 (Fig. 6, *B–D*). Supporting this

model, KSR1 regulation of PKC and ERK signaling but not PKA has been shown elsewhere and knockdown of KSR1 function in null mice interferes with LTP and learning (5).

Stargazin plays a critical role in promoting AMPAR clustering and surface expression through its interaction with AMPARs and PSD95 (23, 24). Our finding that stargazin associates with both GluA1 and GluA4 AMPAR subunits is interesting as it suggests non-selective subunit trafficking. However, the involvement of additional TARPs that convey subunit specificity cannot be excluded. Moreover, the interaction between stargazin and these AMPAR subunits is not modulated by conditioning indicating that this linkage is stable. There are a number of TARPs, and it has been suggested that different TARP subtypes might be used to traffic specific AMPAR subunits (11). While there is evidence for subunit-specific control of lysosomal degradation by stargazin, the exact role of stargazin in synaptic or surface targeting of AMPARs is not completely clear (23, 25). Recent evidence indicates that stargazin may be involved in AMPAR stability once they are delivered to synapses (26). Single particle tracking of AMPARs in cultured hippocampal neurons suggests that a stargazin-PSD95 interaction induced by CaMKII-mediated phosphorylation of stargazin functions to immobilize AMPARs at synapses. From these data, SAP97 may have a primary role in delivery of AMPARs to the PSD during classical conditioning while stargazin, but not SAP97, serves to stabilize them once delivered.

To summarize, these data suggest that SAP97 forms the backbone of a protein scaffold critical for the appropriately timed delivery of AMPARs to the PSD during *in vitro* classical conditioning. Selective chaperoning of GluA1- or GluA4-containing AMPARs is accomplished by individual scaffolding proteins and kinases that are coordinated by SAP97. Together, the findings support our sequential two-stage model of AMPAR synaptic delivery during classical conditioning (7, 8) and reveals a cooperative interaction of multiple scaffolding proteins to selectively deliver subunit-specific AMPARs to the synapse.

Acknowledgments—We thank the anonymous reviewers for suggestions that improved the manuscript.

REFERENCES

1. Colledge, M., Dean, R. A., Scott, G. K., Langeberg, L. K., Huganir, R. L., and Scott, J. D. (2000) Targeting of PKA to glutamate receptors through a MAGUK-AKAP complex. *Neuron* **27,** 107–119
2. Tavalin, S. J., Colledge, M., Hell, J. W., Langeberg, L. K., Huganir, R. L., and Scott, J. D. (2002) Regulation of GluR1 by the A-kinase anchoring protein 79 (AKAP79) signaling complex shares properties with long-term depression. *J. Neurosci.* **22,** 3044–3051
3. Wong, W., and Scott, J. D. (2004) AKAP signaling complexes: Focal points in space and time. *Nat. Rev. Mol. Cell Biol.* **5,** 959–970
4. Nie, T., McDonough, C. B., Huang, T., Nguyen, P. V., and Abel, T. (2007) Genetic disruption of protein kinase A anchoring reveals a role for compartmentalized kinase signaling in theta-burst long-term potentiation and spatial memory. *J. Neurosci.* **27,** 10278–10288
5. Shalin, S. C., Hernandez, C. M., Dougherty, M. K., Morrison, D. K., and Sweatt, J. D. (2006) Kinase suppressor of Ras1 compartmentalizes hippocampal signal transduction and subserves synaptic plasticity and memory formation. *Neuron* **50,** 765–779
6. Zheng, Z., and Keifer, J. (2009) PKA has a critical role in synaptic delivery of GluR1- and GluR4-containing AMPARs during initial stages of acquisition of *in vitro* classical conditioning. *J. Neurophysiol.* **101,** 2539–2549
7. Keifer, J., and Zheng, Z. (2010) AMPA receptor trafficking and learning. *Eur. J. Neurosci.* **32,** 269–277
8. Zheng, Z., Sabirzhanov, B., and Keifer, J. (2012) Two-stage AMPA receptor trafficking in classical conditioning and selective role for glutamate receptor subunit 4 (tGluA4) flop splice variant. *J. Neurophysiol.* **108,** 101–111
9. Zheng, C. Y., Seabold, G. K., Horak, M., and Petralia, R. S. (2011) MAGUKs, synaptic development, and synaptic plasticity. *Neuroscientist* **17,** 493–512
10. Leonard, A. S., Davare, M. A., Horne, M. C., Garner, C. C., and Hell, J. W. (1998) SAP97 is associated with the α-amino-3-hydroxy-5-methylisoxazole-4-propionic acid receptor GluR1 subunit. *J. Biol. Chem.* **273,** 19518–19524
11. Greger, I. H., Ziff, E. B., and Penn, A. C. (2007) Molecular determinants of AMPA receptor subunit assembly. *TINS* **30,** 407–416
12. Granger, A. J., Shi, Y., Lu, W., Cerpas, M., and Nicoll, R. A. (2013) LTP requires a reserve pool of glutamate receptors independent of subunit type. *Nature* **493,** 495–500
13. Anderson, C. W., and Keifer, J. (1999) Properties of conditioned abducens nerve responses in a highly reduced *in vitro* brain stem preparation from the turtle. *J. Neurophysiol.* **81,** 1242–1250
14. Mokin, M., and Keifer, J. (2006) Quantitative analysis of immunofluorescent punctate staining of synaptically localized proteins using confocal microscopy and stereology. *J. Neurosci. Meth.* **157,** 218–224
15. Gardner, L. A., Naren, A. P., and Bahouth, S. W. (2007) Assembly of an SAP97-AKAP79-cAMP-dependent protein kinase scaffold at the type 1 PSD-95/DLG/ZO1 motif of the human β1-adrenergic receptor generates a receptosome involved in receptor recycling and networking. *J. Biol. Chem.* **282,** 5085–5099
16. Zheng, Z., and Keifer, J. (2008) Protein kinase C-dependent and independent signaling pathways regulate synaptic GluR1 and GluR4 AMPAR subunits during *in vitro* classical conditioning. *Neurosci.* **156,** 872–884
17. Yu, W., Fantl, W. J., Harrowe, G., and Williams, L. T. (1998) Regulation of the MAP kinase pathway by mammalian KSR through direct interaction with MEK and ERK. *Curr. Biol.* **8,** 56–64
18. Cacace, A. M., Michaud, N. R., Therrien, M., Mathes, K., Copeland, T., Rubin, G. M., and Morrison, D. K. (1999) Identification of constitutive and ras-inducible phosphorylation sites of KSR: Implications for 14-3-3 binding, mitogen-activated protein kinase binding, and KSR overexpression. *Mol. Cell Biol.* **19,** 229–240
19. Li, W., and Keifer, J. (2009) BDNF-induced synaptic delivery of AMPAR subunits is differentially dependent on NMDA receptors and requires ERK. *Neurobiol. Learn. Mem.* **91,** 243–249
20. Sun, X., Zhao, Y., and Wolf, M. E. (2005) Dopamine receptor stimulation modulates AMPA receptor synaptic insertion in prefrontal cortex neurons. *J. Neurosci.* **25,** 7342–7351
21. Oh, M. C., Derkach, V. A., Guire, E. S., and Soderling, T. R. (2006) Extrasynaptic membrane trafficking regulated by GluR1 serine 845 phosphorylation primes AMPA receptors for long-term potentiation. *J. Biol. Chem.* **281,** 752–758
22. Yang, Y., Wang, X., Frerking, M., and Zhou, Q. (2008) Delivery of AMPA receptors to perisynaptic sites precedes the full expression of long-term potentiation. *Proc. Natl. Acad. Sci. U.S.A.* **105,** 11388–11393
23. Nicoll, R. A., Tomita, S., and Bredt, D. S. (2006) Auxiliary subunits assist AMPA-type glutamate receptors. *Science* **311,** 1253–1256
24. Bats, C., Groc, L., and Choquet, D. (2007) The interaction between stargazin and PSD-95 regulates AMPA receptor surface trafficking. *Neuron* **53,** 719–734
25. Kessels, H. W., Kopec, C. D., Klein, M. E., and Malinow, R. (2009) Roles of stargazin and phosphorylation in the control of AMPA receptor subcellular distribution. *Nat. Neurosci.* **12,** 888–896
26. Opazo, P., Labrecque, S., Tigaret, C. M., Frouin, A., Wiserman, P. W., De Koninck, P., and Choquet, D. (2010) CaMKII triggers the diffusional trapping of surface AMPARs through phosphorylation of stargazin. *Neuron* **67,** 239–252